ELSEVIER

Biophysical Chemistry 108 (2004) 273–279

Biophysical Chemistry

www.elsevier.com/locate/bpc

Sedimentation velocity, multi-speed method for analyzing polydisperse solutions

Walter F. Stafford[a,*], Emory H. Braswell[b]

[a]*Analytical Ultracentrifugation Research Laboratory, Boston Biomedical Research Institute, 64 Grove Street, Watertown, MA 02472, USA*

[b]*National Analytical Ultracentrifugation Facility, University of Connecticut, Storrs, CT 06269-3149, USA*

Abstract

A method is described for the sedimentation velocity analysis of solutions composed of macromolecular solutes of widely disparate size. In sedimentation velocity experiments, usually a single rotor speed is chosen for the entire run, and consequently, the range of observable sedimentation coefficients can be severely limited. This limitation can be removed if the speed is varied during the run, starting with a relatively low speed so that the largest particles can be easily observed. The speed is increased during the run until full speed is attained and the run continued at full speed until the smallest species of interest have cleared the solution. The method, called wide distribution analysis, is based on the method developed originally by Yphantis and co-workers (Proc. Natl. Acad. Sci. USA 78 (1981) 1431) and on the time derivative method of Stafford (Anal. Biochem. 203 (1992) 295), essentially eliminating both the time-independent and radially-independent noise thereby improving the precision, especially for interference optics. An algorithm for analysis of data from both absorbance and interference optics and experimental protocols compatible with the Beckman XL-I Analytical Ultracentrifuge are presented. With these protocols an extremely wide range of sedimentation coefficients from approximately 1.0 to 250 000 S can be accommodated in a single multi-speed run.

Keywords: Sedimentation velocity; Sedimentation coefficients; Wide distribution analysis

1. Introduction

Quantitative characterization of solutions of molecules which are highly heterogeneous with respect to size is of great interest to pharmaceutical and biotechnology firms. In sedimentation velocity experiments, usually a single rotor speed is chosen for the entire run, and consequently, the range of observable sedimentation coefficients can be severely limited. For example, at 50 000 rpm at the usual acceleration rate of 400 rpm/s, the largest particle that would be half way down the cell would have a sedimentation coefficient of only approximately 280 S. This limitation can be removed and the range expanded by approximately three orders of magnitude, if the speed is varied during the run, starting with a relatively low speed so that the largest particles can be easily observed. The speed is increased during the run until full speed is attained and the run continued at full speed until the smallest species of interest have

*Corresponding author. Tel.: +1-617-658-7808; fax: +1-617-972-1753.

E-mail address: stafford@bbri.org (W.F. Stafford).

0301-4622/04/$ - see front matter © 2003 Elsevier B.V. All rights reserved.
doi:10.1016/j.bpc.2003.10.027

cleared the solution. The data from each speed are combined into a single continuous distribution function.

A sedimentation velocity technique developed by Yphantis and co-workers [1] follows changes in the concentration of the solution with time at one point in the cell, while the speed is increased. Machtle [2] used the term 'gravitational sweep' to describe size distribution studies of large particles by sedimentation velocity in which the rotor speed is also varied. He has more recently improved the technique [3]. The gravitational sweep technique was implemented in his laboratory at BASF in the early 1970s (Machtle, personal communication).

The current method is based on the one developed by Yphantis and co-workers but can follow the change in concentration at multiple radial positions simultaneously. The method of data analysis is based on the time derivative method developed by Stafford [4], essentially eliminating both the time-independent and radially-independent noise thereby improving the precision, especially for interference optics.

A program for analysis of data from both absorbance and interference optics and experimental protocols compatible with the Beckman XL-I Analytical Ultracentrifuge are presented.

2. Theoretical background

The time derivative, $(\partial c/\partial s^*)_r$, is computed directly from an array of $c(r, t)$ vs. $s^*(r, t)$ at each radial position, r, that is chosen for the analysis. Typically, the positions chosen are from 6.0 to 7.1 cm in increments of 0.1 cm. The distribution function computed from the time derivative is given by [5]

$$g(s^*) \equiv \left(\frac{\partial c}{\partial s^*}\right)_t = \left[\left(\frac{\partial c}{\partial t}\right)_r - \left(\frac{\partial c}{\partial t}\right)_{s^*}\right]\left(\frac{\partial t}{\partial s^*}\right)_r \tag{1}$$

where $c = c(r, t)$, and since

$$\left(\frac{\partial c}{\partial s^*}\right)_r = \left(\frac{\partial c}{\partial t}\right)_r \left(\frac{\partial t}{\partial s^*}\right)_r, \tag{2}$$

$$g(s^*) = \left(\frac{\partial c}{\partial s^*}\right)_r - \left(\frac{\partial c}{\partial t}\right)_{s^*}\left(\frac{\partial t}{\partial s^*}\right)_r \tag{3}$$

We can approximate the derivative of the concentration at each radial position with respect to s^* by

$$\left(\frac{\partial c}{\partial s^*}\right)_r \approx \frac{\Delta c}{\Delta s^*} = \frac{c(t_2,\ r_1) - c(t_1,\ r_1)}{s^*(t_2,\ r_1) - s^*(t_1,\ r_1)} \tag{4}$$

where

$$s^*(t_i,\ r_j) = \frac{1}{\omega^2 t_i} \ln\left(\frac{r_j}{r_{\text{men}}}\right) \tag{5}$$

and, where r_j is a particular radius selected for the analysis.

As noted previously [5]

$$\left(\frac{\partial c}{\partial t}\right)_{s^*} \approx -2\omega^2 \int_{s^*=0}^{s^*} s^* \hat{g}(s^*) \mathrm{d}s^* \tag{6}$$

and so we arrive at the final relation from which the distribution function is computed.

$$\hat{g}(s^*) = \left(\frac{\partial c}{\partial s^*}\right)_r + \left(2\omega^2 \int_{s^*=0}^{s^*=s^*} s^* \hat{g}(s^*) \mathrm{d}s^*\right)\left(\frac{\partial t}{\partial s^*}\right)_r \tag{7}$$

Since $g(s^*)$ is a function of itself, this relation must be evaluated by iteration. The value of $(\partial t/\partial s^*)_r$ is obtained by implicit differentiation of Eq. (5) and is just $(-t/s^*)$.

The resulting analysis can be plotted either as $g(s^*)$ vs. s^* if the range of s^* values is relatively small or as $s^* \cdot g(s^*)$ vs. $\ln(s^*)$ if the range is large. The areas under the peaks on either scale give the concentration for the boundary corresponding to each peak in the distribution.

3. The method

3.1. Removal of systematic noise

There are two types of systematic noise that must be removed from the data before they can be

Table 1
Typical speed ramping protocol

Speed (rpm)	Time at each speed (s)	$\int(\omega^2 dt)$ ($\times 10^{-8}$/s)	s^* (at 6.5 cm) (svedbergs)[a]	$\ln(s^*)$ (at 6.5 cm)
0–6000[b]	15	0.020	506 606	13.1
6000	600	2.388	4223	8.35
9000	600	7.718	1299	7.17
13 000	600	18.83	550	6.31
18 000	600	40.16	249	5.51
25 000	600	81.28	123	4.81
35 000	600	161.86	62	4.12
50 000	3600	326.38	31	3.42
50 000	3600	1313.3	7.6	2.03
50 000	3600	2300.3	4.4	1.47
50 000	3600	3287.3	3.0	1.11
50 000	3600	4274.28	2.3	0.85

Assuming radius of the meniscus = 5.9 cm.
[a] s^* (6.5 cm) = $\ln(6.5/5.9)/\int(\omega^2 dt)$.
[b] Acceleration phase at the default rate of 400 rpm/s for the XL-I using 1/3 the time to accelerate to 6000 rpm.

analyzed: the first, common to both absorbance and interference optics, is time-independent, radially-dependent background variations that arise from dirt, oil and inhomogeneities in the optics. Since this type of noise is time invariant, it can be completely removed from the data by taking the time derivative of the data. The other type of noise is radially independent but variable over time. It is mainly associated with interference optics and results from slight movements and flexing of the optical system, resulting in small vertical displacements of the interference pattern; this type of noise can be removed by aligning the scans in a region where no sedimentation is taking place, typically in the air space centripetal to both the solvent and solution menisci. These two alignment steps have been implemented previously in DCDT [4], ABDC_Fitter [6] and SEDANAL [8].

3.2. Speed variation protocol

Table 1 suggests a speed ramping protocol that would give a range from over 200 000 S to less than 2.0 S in a single experiment. The machine would be run for 600 seconds at each speed until full speed of 50 000 rpm; thereafter, the machine would be run at 50 000 until the smallest material had sedimented more than half way to the bottom. The number of scans taken at each speed depends on the optical system in use. The slowness of the current absorbance scanning mechanism would allow only 5–10 scans during each 600-second period. The recommended protocol for absorbance optics is to take at least 10 scans at each speed with a point density of 0.003–0.005 cm per point and an average of four lamp flashes.

3.3. Variation of meniscus position with speed

The meniscus position generally is dependent upon speed. At low speeds the meniscus can be quite curved such that its average position is significantly different from its position at higher speeds. As the speed increases the meniscus becomes flattened and moves to higher radius. In addition to the flattening of the meniscus, the rotor will both stretch and shift its position as the speed is changed. Rotor stretching is different for the four- and eight-hole rotors. Table 2 shows typical values of the meniscus radius as a function of speed with a four-hole rotor. The software (DCDT or SEDANAL) requires the user to choose the meniscus position at each speed.

3.4. Optical blank correction

With a shifting center of rotation, optical blank subtraction becomes a problem. Therefore, a

Table 2
Typical variation of meniscus position with speed for a four-hole titanium rotor

Speed (rpm)	R (cm)
12 000	5.9038
18 000	5.9167
25 000	5.9204
35 000	5.9263
50 000	5.9413

machine optical blank is taken in the scallop of the four-hole rotor or in an empty hole in the eight-hole rotor. The effect of the difference in window distortions as the speed is changed cannot be taken into account but does not appear to be a serious problem since it affects only small regions of the distribution function corresponding to the speed change.

4. Experimental

4.1. Materials and methods

The three samples used were: (1) *Limulus polyphemus* hemocyanin, dialyzed against 0.05 m Tris−HCl + 20 mM $CaCl_2$ at pH 7.0, (2) polybead polystyrene 0.11-μm microspheres certified standard (Cat #21755) and (3) polybead polystyrene 0.057-μm microspheres (Cat #08691). The latter two were supplied by Polysciences Inc., at a stock concentration of ~25 mg/ml. Interference velocity sedimentation experiments were performed with a Beckman XL-I Analytical Ultracentrifuge (UC) using the following three solutions: (1) hemocyanin at 2 mg/ml, (2) a mixed solution of the two polystyrene bead samples at 0.5 mg/ml each and (3) a solution containing hemocyanin (2 mg/ml) and the two polystyrene bead samples (0.5 mg/ml each).

All the samples were diluted to their final concentrations with the dialysate buffer from the final dialysis of the hemocyanin. The dialysate buffer was also used as the reference solvent for the interference studies in the double sector velocity UC cells, which were fitted with sapphire windows. The solution in the sample sector was leveled with that in the solvent sector in usual manner [7]. The cells were then placed in the rotor, equilibrated to 20 °C, after which the rotor velocity was ramped through the speeds of 12, 18, 25, 35 and 50 krpm, and between 50 and 90 scans were made at each speed (~20 min) except at the highest speed. The run was continued at 50 k until it was obvious that the solution was cleared of protein at radii in the lower half of the cell. In this case the run was held at 50 k for 3 h in order to bring most of the 5 S material to the lower quarter of the cell. Obviously, if the slowest sedimenting material had a s value greater than 5 S, less time would be necessary at the highest speed.

The software performs the analysis simultaneously at 0.1 cm increments from the meniscus to the base. The choice of radius at which to display the analysis will be a compromise between resolution and one's being able to include the slowest material. The choice of radii near the bottom will afford the greatest resolution but may exclude the more slowly sedimenting species from the curve. Conversely, the choice of a radius in the upper third of the cell might include the smallest species present but will give lower resolution than if a higher radius had been chosen. The resolution increases roughly as the square root of the distance traveled.

5. Results

Analysis proceeded as outlined above, utilizing the 'wide distribution analysis' (WDA) method included as part of the DCDT algorithm in the SEDANAL program [8]. Results utilizing the data at two radii (6.6 and 6.7 cm) overlaid quite well (not shown). As can be seen in Fig. 1, the hemocyanin sample resolved into four peaks (s values of ≈5, 16, 40 and 60 S) corresponding to monomers, hexamers, 24-mers and 36-mers. The solution containing the two sizes of polystyrene beads resolved (Fig. 2) as expected into two components (s values of ≈88 and 350 S). The solution that resulted from the mixture of hemocyanin and the two types of polystyrene beads resolved (Fig. 3) into the usual four hemocyanin peaks, and instead of the expected two additional peaks due to the polystyrene, there resulted a broad distribution with a small peak at ~221 S, a shoulder at 665 S and a broad peak at 1100 S. It appears that a reaction

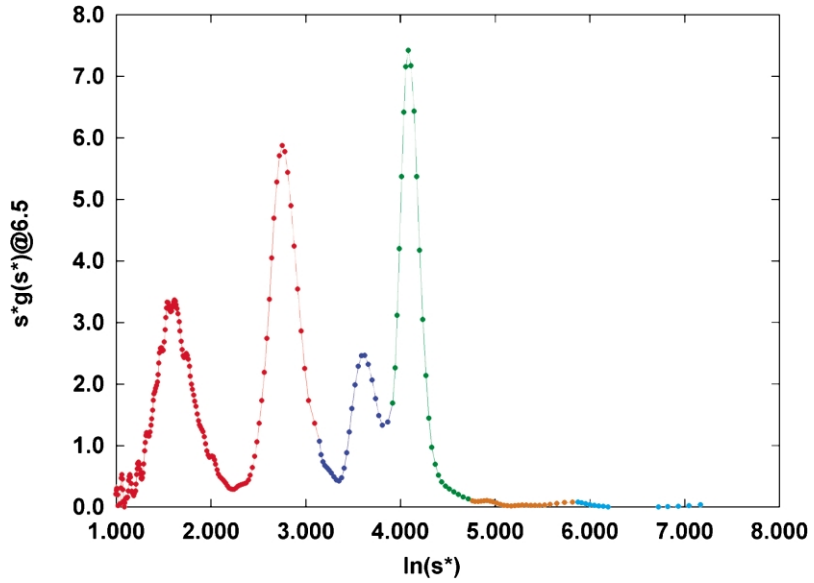

Fig. 1. Plot of $s \cdot g(s^*)$ vs. $\ln(s^*)$ for a hemocyanin solution (2 mg/ml) centrifuged for approximately 20 min at each speed before ramping to the next speed (see text for run conditions). The points acquired at each speed are shown in a different color.

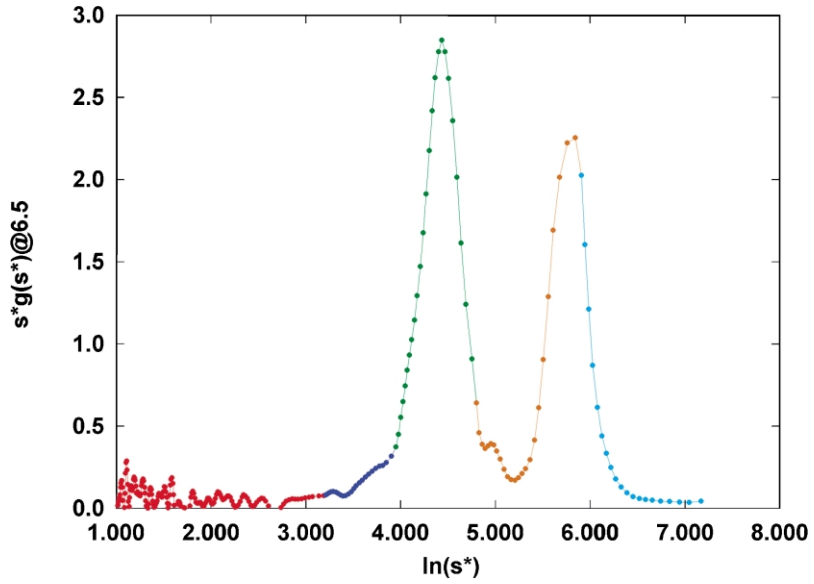

Fig. 2. Suspension of two sizes (0.11- and 0.057-μm diameter) of polystyrene beads (each at 0.5 mg/ml) centrifuged in a similar manner.

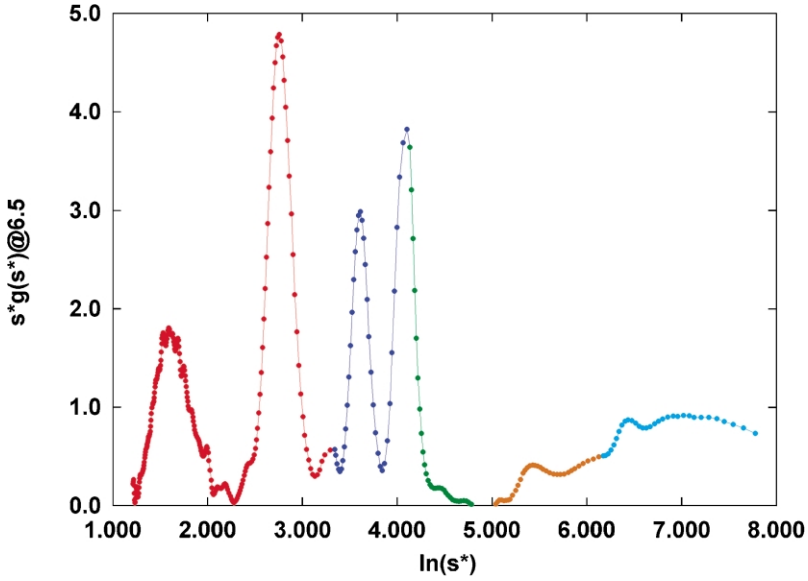

Fig. 3. A mixture of hemocyanin (2 mg/ml) and two sizes of polystyrene beads (each at 0.5 mg/ml) centrifuged in a similar manner.

between the beads and hemocyanin has occurred because all of the polystyrene has disappeared producing large aggregates with a broad size distribution. Careful examination shows that the amounts of material in each of the hemocyanin peaks has been reduced, while that of the 60 S peak was reduced the most. A more detailed examination of the relative areas was not attempted because the various hemocyanin peaks may have been in equilibrium with each other, but one can conclude that the beads were totally saturated and that several protein molecules must bind to each polystyrene bead including some which bridge between beads leading to the very large aggregates observed.

6. Conclusions

A multi-speed, WDA method for analysis of polydisperse macromolecular samples having a wide distribution of sedimentation coefficients has been developed and tested. The rotational speed is varied during the run to achieve a wide range of gravitational field strengths allowing the analysis of a wide range of macromolecular size. In a single experiment, by starting at very low speeds (2000–3000 rpm), a sample containing material with sedimentation coefficients ranging from 2 S up to more than 250 000 S can be accommodated. Software for WDA analysis can be found on the RASMB FTP server at ftp://rasmb.bbri.org.

Acknowledgments

We thank Eric Anderson for performing the sedimentation runs and Jeff Lary for data analysis and software development. This work was in part supported by a grant from the National Science Foundation to WFS (#BIR-9513060) and NSF 9318373 to the National Analytical Ultracentrifuge Facility at the University of Connecticut.

References

[1] M.S. Runge, T.M. Laue, D.A. Yphantis, et al., ATP-induced formation of an associated complex between microtubules and neurofilaments, Proc. Natl. Acad. Sci. USA 78 (1981) 1431–1435.
[2] W. Machtle, Characterization of dispersions using combined H_2O/D_2O ultracentrifuge measurements, Mak-

romol. Chem.-Macromol. Chem. Phys. 185 (1984) 1025–1039.
[3] W. Machtle, High-resolution, submicron particle size distribution analysis using gravitational-sweep sedimentation, Biophys. J. 76 (1999) 1080–1091.
[4] W.F. Stafford, Boundary analysis in sedimentation transport experiments: a procedure for obtaining sedimentation coefficient distributions using the time derivative of the concentration profile, Anal. Biochem. 203 (1992) 295–301.
[5] W.F. Stafford, Analysis of reversibly interacting macromolecular systems by time derivative sedimentation velocity, Methods Enzymol. 323 (2000) 302–325.
[6] W.F. Stafford, Time difference sedimentation velocity analysis of rapidly reversible interacting systems: determination of equilibrium constants by non-linear curve fitting procedures, Biophys. J. 74 (1998) A301.
[7] W.F. Stafford, Analytical ultracentrifugation, in: J.E. Coligan, B.M. Dunn, H.L. Ploegh, D.W. Speicher, P.T. Wingfield (Eds.), Current Protocols in Protein Science, Wiley, New York, 2003, pp. 20.7.1–20.7.10.
[8] W.F. Stafford, P.J. Sherwood, Analysis of heterologous interacting systems by sedimentation velocity: curve fitting algorithms for estimation of sedimentation coefficients, equilibrium and kinetic constants, Biophys. Chem. 108 (2003) 231–243.